J Biorheol (2011) 25:18–26
DOI 10.1007/s12573-011-0032-5

ORIGINAL ARTICLE

Impaired deformability of erythrocytes in diabetic rat and human: investigation by the nickel-mesh-filtration technique

K. Saito · Y. Kogawa · M. Fukata · K. Odashiro · Toru Maruyama · K. Akashi · T. Fujino

Received: 1 October 2010 / Accepted: 27 April 2011 / Published online: 20 May 2011
© Japanese Society of Biorheology 2011

Abstract Comprehensive research to quantify the deformability of erythrocytes in diabetic animals and humans has been lacking. The objective of this study was to compare the impairment of erythrocyte deformability in diabetic rats and patients by use of the same rheologic method. Deformability was investigated in streptozotocin-induced diabetic rats and diabetic patients, by using the highly sensitive and quantitative nickel-mesh-filtration technique. Erythrocyte filterability (whole-cell deformability) was defined as flow rate of hematocrit-adjusted erythrocyte suspension relative to that of saline (%). Hematological and biochemical data for diabetic rats did not differ from those for age-matched control rats except for hyperglycemia and malnutrition. Erythrocyte filterability for diabetic rats was significantly lower than that for control rats ($69.4 \pm 10.1\%$, $n = 8$, compared with $83.1 \pm 4.2\%$, $n = 8$; $p < 0.001$). Likewise, erythrocyte filterability for diabetic patients was significantly impaired compared with that for controls ($87.6 \pm 3.4\%$, $n = 174$, compared with $88.6 \pm 2.1\%$, $n = 51$; $p = 0.046$). Stepwise multiple regression analysis revealed that this impairment was mostly attributable to associated obesity (BMI, $p = 0.029$) and glycemic stress (HbA1c(JDS), $p = 0.046$). We therefore conclude that erythrocyte filterability is commonly impaired in diabetic rats and in humans. Moreover, metabolic risk accumulation further impairs erythrocyte filterability, resulting in derangement of the microcirculation.

Keywords Deformability · Diabetic patient · Diabetic rat · Erythrocytes · Filtration · Microcirculation · Nickel-mesh

K. Saito
BOOCS Clinic, Fukuoka, Japan

Y. Kogawa · M. Fukata · K. Odashiro · K. Akashi
Department of Medicine, Kyushu University, Fukuoka, Japan

T. Maruyama (✉)
Institute of Health Science, Kyushu University,
Kasuga Kohen 6-1, Kasuga 816-8580, Japan
e-mail: maruyama@ihs.kyushu-u.ac.jp

T. Fujino
Institute of Rheological Function of Foods Co. Ltd,
Hisayama, Japan

Introduction

It is well known that the microcirculation becomes progressively impaired in diabetes mellitus, which is characterized by diabetic microangiopathy. This diabetic environment is believed to have a rheologic effect on circulating erythrocytes. Although erythrocyte rheology in diabetes has been widely investigated, the results have been confusing because of diverse rheologic methodologies with different sensitivity and limited reproducibility [1].

The deformability of erythrocytes that pass through the microvascular network is an essential factor affecting physiological microcirculation. However, the concept of erythrocyte deformability has not been strictly defined as a physical quantity, and evaluation of deformability depends on the measurement technique and its relative sensitivity. Because in-vivo erythrocyte deformation involves bending, erythrocyte deformability can be quantified by measuring erythrocyte filterability (whole cell deformability), by use of the highly sensitive and quantitative nickel-mesh-filtration technique, which is useful for assessing the physiological bending deformation of intact circulating erythrocytes [2–4].

To date, comprehensive research to quantify impaired erythrocyte deformability in a diabetic model and in humans using the same rheologic method has been lacking. Therefore, we investigated the effect of diabetes on erythrocyte rheology by using the nickel-mesh-filtration technique to examine suspensions of erythrocytes obtained from rats treated with streptozotocin (STZ) and those obtained from diabetic patients.

Materials and methods

Animals

Animal care and use have been described elsewhere in detail [5]. Ten-week-old male Wistar–Kyoto rats (WKY; Charles River Japan, Tsukuba, Japan) were treated according to the Principles of Laboratory Animal Care published by the NIH (1985), i.e., rats were housed for 1 week in metal cages in a temperature-controlled room (21 ± 0.5°C) and maintained on a standard commercial rat chow and water ad libitum. Light/dark cycle was 7:00 am and 19:00 pm. Diabetes was induced in the rats when 11 weeks old by single injection of STZ (Sigma Chemicals, St Louis, MO, USA) into the tail vein (65 mg/kg) under ether anesthesia (Wako, Osaka, Japan) and pentobarbital (40 mg/kg; Abbott Laboratory, Chicago, IL, USA). STZ was dissolved in citrate buffer (0.05 mol/l, 0.8 ml/kg, pH 4.5) immediately before injection. Untreated WKY rats were used as age-matched controls. Plasma glucose concentration was estimated (Fujichem 1000; Fuji Film, Tokyo, Japan) before and after STZ injection by blood sampling from the tail vein to confirm the diabetic condition. Under the same anesthesia, blood was sampled from the abdominal aorta from 13-week-old rats before sacrifice in order to prepare erythrocyte suspensions.

Human subjects

The human study was performed according to the Declaration of Helsinki (2000), i.e., signed informed consent was obtained from each subject before enrollment into the study. The study population consisted of 174 Japanese patients with type 2 diabetes mellitus and 51 non-diabetic control subjects. Diabetic patients were treated at the discretion of the treating physicians in outpatient clinics within or in the vicinity of Fukuoka City. Diabetic complications were evaluated by experienced diabetologists and ophthalmologists. Medications and life style including smoking were not altered in any patient during the study period. The human and animal study designs were approved by the internal ethics committee of The Institute of Rheological Function of Foods (Hisayama, Fukuoka, Japan).

Erythrocyte suspensions

Erythrocyte suspensions were prepared as described elsewhere [5, 6]. For rats, blood was sampled by puncturing the abdominal aorta via laparotomy after a 12-h fast using 21-gauge needles and disposable syringes (Terumo Japan, Tokyo, Japan) filled with 1/10 volume of 3.8% trisodium citrate as anticoagulant. For human subjects, approximately 10 ml venous blood was drawn from the antecubital vein using needles and syringes identical with those used for rats. Venous blood sampling was performed in the morning after an overnight fast.

Blood cell counting and hematocrit measurements were carried out using a hemocytometer (Ace Counter, FLC-240A; Fukuda Denshi, Tokyo, Japan). After centrifugation at 1300×*g* for 10 min, supernatant was carefully aspirated to replace buffy coat and plasma with saline buffered with *N*-(2-hydroxyethyl)piperazine-*N*′-2-ethanesulfonic acid (HEPES) sodium salt (HEPES-Na). Composition of HEPES-Na-buffered saline (HBS) was NaCl 141 mM and HEPES-Na 10 mM. Osmolality and pH of the HBS were 287 mOsm/kg H_2O and 7.4, respectively. The osmolality of the HBS was measured using a freezing point depression type osmometer (Fiske Mark 3 Osmometer, Fiske Associates, MA, USA). Erythrocytes were then washed three times by repeated resuspension with HBS and centrifugation at 800×*g*, 600×*g*, and 500×*g*, each for 10 min. The final hematocrit of human erythrocyte suspension was adjusted to 3.0% and that of rat erythrocyte suspension was adjusted to 2.0% because of limited blood sample volume. These procedures were performed within 2 h after blood sampling for subsequent filtration experiments.

Nickel-mesh filter

Figure 1a shows an electron microscopic photograph of a nickel-mesh filter that was produced in accordance with our specifications by a photofabrication technique (Dainippon Printing, Tokyo, Japan). We specified that this filter should have an outer diameter of 13 mm, a filtration area 8 mm in diameter, and be 11 μm thick with an interpore distance of 35 μm (Tsukasa Sokken, Tokyo, Japan). The vertical and cylindrical pores were distributed regularly across the filter without coincidence or branching. The pore entrances were round, and resulted in smooth transition into the pore interior. Pore diameters are all exactly identical in a specific nickel-mesh filter. Filters with a specific pore diameter ranging from 3.0 to 6.0 μm are available for selection on the basis of the suspension materials. After repeated preliminary experiments to choose an appropriate pore size, a nickel-mesh filter with a pore diameter of 3.85 μm was chosen for rats and one with a pore diameter of 4.94 μm for humans, taking the species-specific

difference between mean corpuscular volume (MCV) of the erythrocytes into account.

Erythrocyte filterability

Filtration experiments were performed blindly using a gravity-based nickel-mesh filtration apparatus (model NOBU-II; Tsukasa Sokken) as shown in Fig. 1b. In brief, the relationship between hydrostatic pressure (P; mmH_2O) and time (t; s) was obtained during continuous filtration by gravity using a pressure transducer. P was transformed to the height of the meniscus in vertical tube (h; mm). The tangent to the h–t curve determined by drawing points corresponding to different heights gives the rate of fall of the meniscus (dh/dt). Thereafter, by multiplying the rate of fall by the internal cross-sectional area of the vertical tube, the complete set of flow rates (Q; ml/min) and corresponding P, the P–Q relationship, was obtained [7, 8]. This procedure was automatically performed by measurement software installed in a personal computer (DELL Latitude CS; Dell, Round Rock, TX, USA) and monitored on the main window of the computer screen. Together with the start of data acquisition, the measurement software displays the h–t curve continuously during the filtration process. When filtration is complete, the software displays the relationship between pressure and flow rate (P–Q curve). The h–t and P–Q curves are shown on the computer screen and stored simultaneously on Microsoft Office Excel 2003 running under Windows XP (Microsoft, Tokyo, Japan). The temperature of the specimens was kept at 25°C by circulating isothermal water through a water jacket surrounding the vertical tube (Fig. 1b). The flow rate of the erythrocyte suspension as a percentage of that of HBS at 100 mmH_2O was used as an index of erythrocyte filterability. These experiments were performed at room temperature (22 ± 3°C).

Erythrocyte shape

An aliquot of the erythrocyte suspension was fixed with isotonic 1.0% glutaraldehyde solution containing 24.5 mM NaCl and 50 mM phosphate buffer (pH 7.4). The shape of erythrocytes was then observed using a differential interference contrast microscope (Diaphoto 300; Nikon, Tokyo, Japan) at 400× magnification.

Data analysis

All data were expressed as mean ± SD. For statistical analysis, human sample size was chosen to provide 90% power with α error of 0.05, and should have been ≥188 cases. The Kolmogorov–Smirnov test was used to confirm the normal distribution of erythrocyte filterability (%) before the intergroup comparison. Continuous variable comparison between two groups was conducted with the unpaired Student's t test, and that among more than two groups was performed by analysis of variance (ANOVA). Discrete variables were analyzed as a contingency table using Fisher's exact test or Pearson's χ^2 test with Yete's continuity correction, if necessary. Stepwise multiple

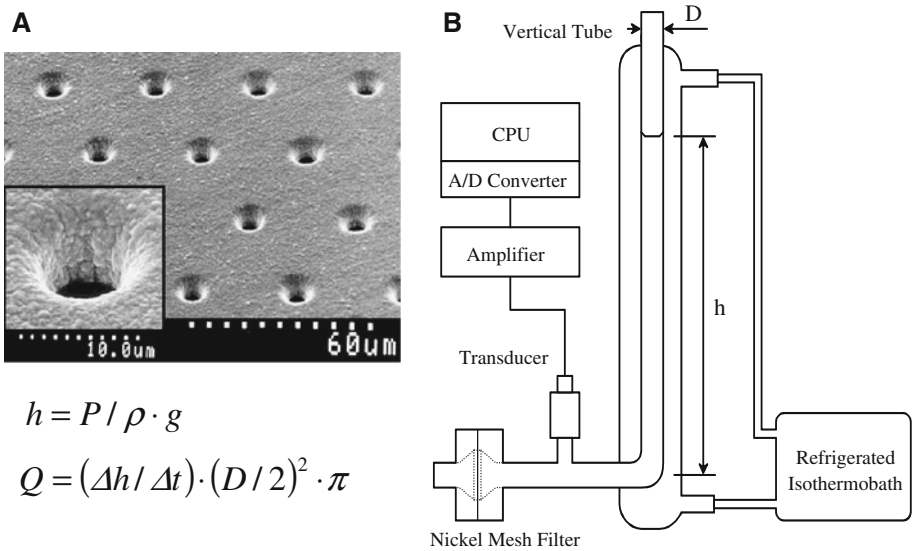

$$h = P / \rho \cdot g$$

$$Q = (\Delta h / \Delta t) \cdot (D/2)^2 \cdot \pi$$

Fig. 1 **a** Scanning electron microscopic photograph of a nickel-mesh filter. Magnification of a single pore in the nickel-mesh shows the smooth transition into the pore interior (*inset*). **b** Schematic illustration of gravity-based nickel-mesh filtration system. The height of the meniscus within the vertical tube (h) was obtained from the continuous decrease of the filtration pressure (P), the specific gravity (ρ), and the acceleration due to gravity (g). Flow rate (Q) was calculated automatically from the first derivative of h with respect to time (dh/dt) and the internal cross sectional area of the vertical tube. D is the internal diameter of the vertical tube

regression analysis was used to determine significant contributors of the erythrocyte filterability impairment. For this regression analysis, antidiabetic treatment was dichotomized as diet therapy, drug therapy, and insulin therapy. Severity of diabetic retinopathy was classified as no retinopathy, simple retinopathy, and proliferative retinopathy. Likewise, diabetic nephropathy was classified as no nephropathy, early nephropathy, overt nephropathy, and renal failure with or without hemodialysis. Further, diabetic neuropathy was classified as no neuropathy, asymptomatic, and symptomatic neuropathy for multiple regression analysis. None of the variables with missing data qualified. The criterion for entry into the regression model was a significant correlation coefficient or otherwise clinically meaningful variables. Possible risk factors were checked for confounding factors and multicollinearity (variance inflation factor >10). These analyses were performed using SPSS software (Windows version 18.0; SPSS, Chicago, IL, USA). Differences with $p < 0.05$ were considered significant.

Results

Animal study

Hematological and biochemical data of STZ-treated 13-week-old diabetic rats ($n = 8$) and age-matched control rats ($n = 8$) are summarized in Table 1. STZ treatment induced severe ($p < 0.001$) hyperglycemia and protein catabolism causing a significant decrease in albumin concentration ($p < 0.001$) and an increase in blood urea nitrogen concentration (BUN, $p < 0.001$). Morphologically, no discernible shape changes were observed for erythrocytes obtained from control and diabetic rats. Figure 2a shows representative *P–Q* curves for saline and for erythrocyte suspensions obtained from control and diabetic rats under continuous filtration. The filtration system contains data-analysis support software installed on a personal computer, which has an option allowing a *P–Q* graphic display and representative point sampling of data acquired during the filtration and access to Microsoft Excel 2003. HBS behaved as a Newtonian fluid, with a linear *P–Q* relationship passing through the origin. The linearity was superimposable indicating excellent reproducibility of this filtration system. In contrast, the *P–Q* relationships for the erythrocyte suspensions were smooth convex curves along the abscissa over the low-pressure region, indicative of non-Newtonian behavior. The flow rate of erythrocyte suspensions from two control rats was greater than that of suspensions from two representative diabetic rats at any given filtration pressure. As summarized in Fig. 2b, erythrocyte filterability for STZ-induced diabetic rats was significantly impaired compared with that for control rats (69.4 ± 10.1%, $n = 8$, compared with 83.1 ± 4.2%, $n = 8$; $p < 0.001$).

Human study

Baseline characteristics for diabetic patients and age-matched control subjects are detailed in Table 2. There were no significant differences between the two groups in blood chemistry except for increases in JDS (Japanese Diabetes Society) value ($p < 0.001$) for hemoglobin A1c (HbA1c(JDS): %) and LDL-cholesterol ($p = 0.024$) in the diabetic group. Hematology showed significantly lower MCV ($p = 0.048$), mean corpuscular hemoglobin (MCH, $p < 0.001$), and mean corpuscular hemoglobin concentration (MCHC, $p < 0.001$) in the diabetic group than in the control group. No outstanding abnormalities of erythrocyte morphology were observed in these two groups. There was a good positive correlation between the concentration (mg/dl) of fasting plasma glucose (y) and HbA1c(JDS) (x) in the diabetic group, yielding a significant linear regression equation ($y = 24.544x - 17.01$, $r = 0.673$, $p < 0.001$).

Table 1 Hematological and biochemical data for control and diabetic rats

	WKY ($n = 8$)	STZ ($n = 8$)	p value
WBC (/μl)	3400 ± 1015	2829 ± 315	0.180
RBC ($\times 10^4$/μl)	751 ± 27	758 ± 41	0.686
Hb (g/dl)	13.2 ± 0.4	13.3 ± 0.7	0.882
Ht (%)	39.9 ± 1.4	39.8 ± 1.9	0.878
MCV (fl)	53.2 ± 1.8	52.5 ± 0.8	0.325
MCH (pg)	17.6 ± 0.6	17.5 ± 0.4	0.648
MCHC (g/dl)	33.1 ± 0.6	33.4 ± 0.6	0.508
Platelets ($\times 10^4$/μl)	76.5 ± 12.9	65.8 ± 8.2	0.089
Total protein (g/dl)	4.6 ± 0.3	4.1 ± 0.4	0.028
Albumin (g/dl)	3.2 ± 0.1	2.8 ± 0.2	<0.001
AST (IU/l)	91.9 ± 9.1	87.0 ± 17.5	0.528
ALT (IU/l)	20.6 ± 8.8	34.4 ± 13.9	0.080
Total cholesterol (mg/dl)	65.7 ± 7.2	65.1 ± 18.1	0.940
HDL cholesterol (mg/dl)	48.4 ± 5.8	47.9 ± 9.0	0.890
LDL cholesterol (mg/dl)	7.3 ± 1.1	9.0 ± 3.9	0.287
Triglyceride (mg/dl)	45.9 ± 14.2	44.4 ± 19.8	0.879
BUN (mg/dl)	14.1 ± 0.8	26.4 ± 2.6	<0.001
Cr (mg/dl)	0.21 ± 0.04	0.19 ± 0.04	0.183
Amylase (IU/l)	556 ± 90	577 ± 105	0.702
Glucose (mg/dl)	114.3 ± 7.7	484.0 ± 118.4	<0.001

ALT alanine aminotransferase, *AST* aspartate transaminase, *BUN* blood urea nitrogen, *Cr* creatinine, *Hb* hemoglobin, *HDL* high density lipoprotein, *Ht* hematocrit, *LDL* low density lipoprotein, *MCH* mean corpuscular hemoglobin, *MCHC* mean corpuscular hemoglobin concentration, *MCV* mean corpuscular volume, *RBC* red blood cells, *STZ* streptozotocin-induced diabetic rats, *WBC* white blood cells, *WKY* Wistar–Kyoto rats

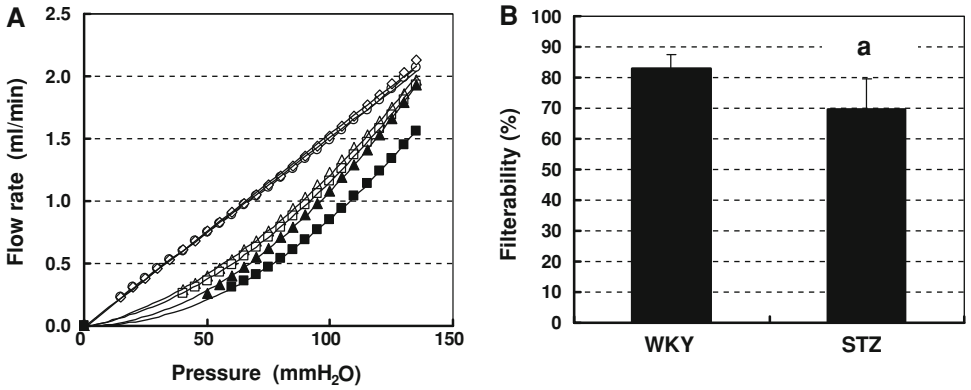

Fig. 2 **a** Representative relationships between filtration pressure (P; mmH_2O) and flow rate (Q; ml/min) during continuous filtration of rat erythrocyte suspensions and HEPES-buffered control saline. The P–Q relationships correspond to two saline passages (*open circles*, *open diamonds*), passages of erythrocyte suspensions from 2 diabetic rats (*filled triangles*, *filled squares*), and those from 2 age-matched control rats (*open triangles*, *open squares*). **b** Summarized data showing difference between erythrocyte filterability for diabetic rats ($n = 8$) and control rats ($n = 8$). *STZ* streptozotocin-induced diabetic rats, *WKY* Wistar–Kyoto rats; [a]$p < 0.001$

Table 2 Clinical baseline characteristics in human diabetic and control groups

	Control group ($n = 51$)	Diabetic group ($n = 174$)	p value
Age (years)	62.6 ± 10.0	60.4 ± 11.2	0.219
Gender (females/males)	22/29	67/107	0.626
BMI (kg/m^2)	23.7 ± 2.9	24.2 ± 3.4	0.421
HbA1c(JDS) (%)	5.20 ± 0.40	7.72 ± 1.80	<0.001
Total cholesterol (mg/dl)	204.5 ± 33.3	211.8 ± 45.1	0.288
HDL cholesterol (mg/dl)	57.2 ± 11.6	55.2 ± 16.3	0.412
LDL cholesterol (mg/dl)	113.9 ± 27.4	125.8 ± 34.5	0.024
Triglyceride (mg/dl)	138.3 ± 87.5	156.7 ± 162.8	0.440
Systolic BP (mmHg)	142.0 ± 16.9	138.5 ± 20.5	0.266
Diastolic BP (mmHg)	81.8 ± 10.3	79.3 ± 11.5	0.176
Hb (g/dl)	14.2 ± 1.6	13.9 ± 1.7	0.260
Ht (%)	40.8 ± 4.3	40.5 ± 4.9	0.757
MCV (fl)	93.1 ± 3.8	91.7 ± 4.5	0.048
MCH (pg)	32.3 ± 1.6	31.3 ± 1.8	<0.001
MCHC (g/dl)	34.7 ± 0.9	34.2 ± 1.0	<0.001
Erythrocyte filterability (%)	88.6 ± 2.1	87.6 ± 3.4	0.046

BMI body mass index calculated by dividing body weight (kg) by the square of height (m), *BP* blood pressure, *HbA1c(JDS)* hemoglobin A1c concentration estimated according to the Japanese Diabetes Society; Other abbreviations are as in Table 1

This indicates that HbA1c(JDS) is a surrogate of glycemic control in the stable diabetic condition under ongoing treatment.

Figure 3a shows representative P–Q relationships for HBS and erythrocyte suspensions obtained from 8 control subjects during filtration experiments. HBS demonstrated linear P–Q relation passing through the origin. P–Q relationships for the erythrocyte suspensions displayed smooth convex curves along the abscissa over the low-pressure region. Figure 3b shows representative P–Q relationships for HBS and erythrocyte suspensions obtained from 8 diabetic patients. The flow rate of erythrocyte suspension in diabetic group was always similar to or less than that of control group (Fig. 3a). The P–Q relationships of obese and non-obese diabetic patients were also compared in Fig. 3b. Note that the flow rate of obese diabetic patients was always less than that of non-obese diabetic patients at any given pressure. Obesity was defined as body mass index (BMI) of 25 or more. BMI was calculated by body weight (kg) divided by square of height (m).

As in Table 2, mean erythrocyte filterability for diabetic patients was slightly but significantly impaired compared with that for control subjects (87.6 ± 3.4%, $n = 174$, compared with 88.6 ± 2.1%, $n = 51$; $p = 0.046$). Table 3 summarizes the correlation between erythrocyte filterability and demographic variables for diabetic patients. The

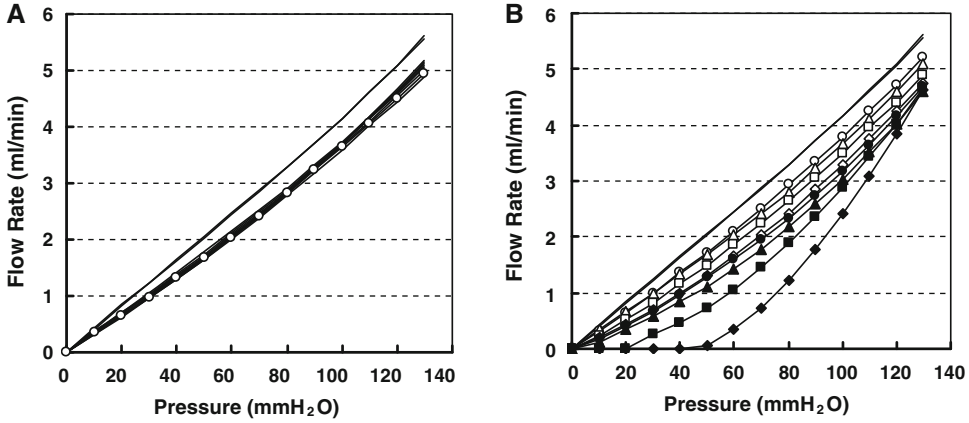

Fig. 3 Representative *P–Q* relationships obtained during continuous filtration of human erythrocyte suspensions. **a** *P–Q* curves for 8 control subjects were quite superimposable. **b** Flow rates for 8 diabetic patients were similar to or less than those for controls at any given filtration pressure. Note that erythrocyte filterability was impaired further in obese (BMI $\geq$ 25) diabetic patients (*filled circles*, *filled triangles*, *filled squares*, *filled diamonds*) relative to non-obese (BMI < 25) diabetic patients (*open circles*, *open triangles*, *open squares*, *open diamonds*)

Table 3 Correlation of erythrocyte filterability and demographic variables in diabetic patients

Continuous data	Correlation coefficient	*p* value
Age (years)	0.082	0.280
BMI (kg/m^2)	−0.206	0.007
HbA1c(JDS) (%)	−0.149	0.050
Total cholesterol (mg/dl)	−0.115	0.132
HDL cholesterol (mg/dl)	0.040	0.602
LDL cholesterol (mg/dl)	−0.144	0.059
Triglyceride (mg/dl)	−0.175	0.022
Systolic BP (mmHg)	0.011	0.883
Diastolic BP (mmHg)	−0.043	0.578
MCV (fl)	0.066	0.386
MCH (pg)	0.050	0.514
MCHC (g/dl)	0.021	0.787
Discrete data	***F* value**	***p* value**
Treatment	0.582	0.560
Diabetic retinopathy	0.933	0.426
Diabetic nephropathy	2.025	0.112
Diabetic neuropathy	0.453	0.636

Abbreviations are as in Tables 1 and 2

respective associations of erythrocyte filterability with BMI ($p = 0.007$) and with serum triglyceride concentration ($p = 0.022$) were significant, whereas the association of the filterability and HbA1c(JDS) was of marginal significance ($p = 0.050$). As in our previous study [6], triglyceride was the only lipid component to have a significant effect on erythrocyte filterability. Neither the respective diabetic complications nor antidiabetic treatments had any significant positive or negative relationship with erythrocyte filterability.

Because diabetic patients have different background characteristics, stepwise multiple regression analysis was performed to find covariates contributing significantly to the impaired erythrocyte filterability with concurrent avoidance of multicollinearity. Significant multiple regression to erythrocyte filterability ($r = 0.289$, $p = 0.030$) was observed for a clinically relevant model including representative variables reflecting background, diabetic control, severity, and complication. In this model, HbA1c(JDS) ($p = 0.046$) and BMI ($p = 0.029$) were significant variables contributing independently to the impaired filterability (Table 4). Although the stepwise reduction method yielded more significant probability ($r = 0.267$, $p = 0.002$), this method reduced the clinical relevance of the regression model.

Discussion

Clinical diabetic studies are always affected by potential confounding factors such as obesity, hypertension and dyslipidemia. Therefore, the preparations used in this study include diabetic rat and human erythrocytes. The main findings of the study are that erythrocyte filterability was significantly impaired in 13-week STZ-induced diabetic rats and in diabetic patients compared with age-matched controls. Stepwise multiple regression analysis showed that impaired diabetic human erythrocyte filterability is mostly attributable to obesity (BMI, $p = 0.029$) and glycemic stress (HbA1c(JDS), $p = 0.046$).

It is generally accepted that erythrocyte deformability is mainly determined by:

1 membrane structure and properties;
2 internal viscosity, which is reflected by MCHC; and

Table 4 Multiple regression analysis predicting contributors to erythrocyte filterability

Covariate	Variance inflation factor	*t* value	*p* value
BMI (kg/m^2)	1.231	−2.206	0.029
Diastolic BP (mmHg)	1.167	−0.137	0.891
MCHC (g/dl)	1.098	0.681	0.497
HbA1c(JDS) (%)	1.124	−2.012	0.046
Triglyceride (mg/dl)	1.130	−1.241	0.216
Nephropathy	1.018	0.323	0.747

Abbreviations are as in Tables 1 and 2

3 cellular geometric factors that are reflected by MCV and erythrocyte shape [3, 7–9].

Therefore, abnormal membrane property, increases in MCHC or MCV, and several kinds of shape changes impair erythrocyte deformability. Because there were no discernible shape changes and equivalent MCV and MCHC in the two rat groups (Table 1), impairment of rat erythrocyte filterability caused by a 2-week diabetic duration mainly arises from erythrocyte membrane properties (Fig. 2). The malondialdehyde content of erythrocytes is reported to increase in STZ-treated rats [10], indicating that erythrocyte membrane damage is partly caused by oxidant stress. In agreement with this, membrane abnormalities of STZ-treated rat erythrocytes have been reported, e.g., Na^+–K^+-ATP_{ase} and Ca^{2+}-ATP_{ase} activities are reduced [11, 12]. These abnormalities affect erythrocyte membrane integrity leading to the impaired deformability, which is a primary rheologic abnormality preceding vascular damage in STZ-induced diabetic rats [13]. Acute exposure of intact erythrocytes to high-glucose media impairs the deformability in a time and concentration-dependent manner [14]. However, this condition may result in intracellular dehydration because of osmotic effects, which also impair the deformability. Therefore, this study using diabetic rats is of note because it shows that in-vivo glycemic stress impairs erythrocyte filterability without any changes in MCV or MCHC (Table 1; Fig. 2). STZ-induced diabetic rats mimic lean diabetic patients under the insulin deficiency and malnutrition. Therefore, the results from the rat study are not necessarily comparable with those from non-uniform diabetic patients.

Erythrocyte deformability is known to be impaired in diabetic patients especially those with diabetic complications. Shin et al. [15] confirmed this findings by ektacytometry, i.e., erythrocyte elongation reflecting deformability was in the order: type 2 diabetic patients with complications < those without complications < controls. Likewise, rheoscopic investigation showed impaired erythrocyte elongation in type 1 diabetic children [16] and laser diffractoscopy demonstrated that erythrocyte elongation was disturbed in type 2 diabetic adults and was improved by antidiabetic drug treatment [17]. However, in-vivo physiological erythrocyte deformation is not elongation but bending. Although rotational techniques causing elongation can determine shear rates, elongation requires severalfold more rheologic stress than bending does, leading to low sensitivity. With regard to the filtration study, use of a conventional filter could not reveal impairment of diabetic erythrocyte filterability [1]. In contrast, this study, using a sensitive, reproducible, and quantitative nickel-mesh filter (Fig. 1a) revealed small but significant impairment of human diabetic erythrocyte filterability (Table 2; Fig. 3). We found significant decreases in MCV and MCHC in the diabetic group compared with the control group, which may have obscured the different erythrocyte filterability (Table 2). Mild impairment of deformability in diabetic patients (Table 2) compared with that in diabetic rats (Table 1) is believed to be partly attributable to therapeutic effects in diabetic patients and an unexpected decrease in MCV and MCHC in diabetic human erythrocytes (Table 2).

Diabetes is considered to have profound and diverse rheologic effects on circulating erythrocytes. Augmented aggregability of erythrocytes in diabetes in the high hematocrit circumstance has complicated interpretation of erythrocyte rheology [18, 19]. However, this study using an erythrocyte suspension with low hematocrit (2.0–3.0%) purely demonstrated impaired diabetic erythrocyte deformability without interaction of the erythrocytes. The main cause of this impairment is believed to be membrane abnormalities of diabetic rat and human erythrocytes. The malondialdehyde content of diabetic rat erythrocytes is increased [10], indicating that hyperglycemia-induced oxidant stress causes erythrocyte membrane lipid peroxidation. Although circulating erythrocytes contain a variety of endogenous antioxidants, our previous studies revealed that the filterability of intact human erythrocytes is markedly impaired by superoxide anion [20], advanced glycation endproducts [21] and *tert*-butyl hydroperoxide [22]. Such acute and profound oxidant stress causes erythrocyte membrane phospholipid peroxidation [23] and protein degradation, leading to increased osmotic fragility [20, 22]. Although oxidant stress in clinical diabetes is relatively mild, persistent and synergistic glycemic and oxidant stress of erythrocytes reduces membrane fluidity [24] leading to the significant rheologic derangement [1, 15–17].

Diabetes contains confounding factors, for example hypertension, dyslipidemia, and obesity, which may affect circulating erythrocyte filterability. Our previous studies using the nickel-mesh filter revealed that dyslipidemia and hypertension have potential effects on filterability [5, 6]. Multiple regression analysis in this study demonstrated that impairment of filterability was mostly attributable to obesity (BMI, $p = 0.029$) and degree of diabetic control

(HbA1c(JDS), $p = 0.046$), suggesting that metabolic risk accumulation causes serious impairment of erythrocyte filterability, resulting in damage to the microcirculation (Fig. 3; Table 4). Metabolic syndrome is also characterized by elevated oxidant stress, which leads to systemic micr-oinflammation [25, 26]. This supports the recent findings from other laboratories, which demonstrated that metabolic syndrome alters erythrocyte membrane properties [27] and impairs erythrocyte deformability [28], resulting in disturbances in microcirculation [29, 30].

In conclusion, this study using a nickel-mesh-filtration technique quantified the filterability of diabetic rat and human erythrocytes. Erythrocyte filterability was commonly impaired in STZ-induced diabetic rats and in type 2 diabetic patients under treatment, and the extent of impairment was severe in the former and mild in the latter. With regard to diabetic patients, multiple regression analysis in this cross sectional study demonstrated that impaired diabetic erythrocyte filterability was mostly attributable to associated obesity and glycemic stress, although a large cohort is required. Finally, this study suggests that metabolic risk accumulation seriously deranges erythrocyte rheology and disturbs microcirculation.

Acknowledgments The authors would like to thank staff of the Institute of Rheological Function of Foods Co. Ltd. (Hisayama, Fukuoka) for technical assistance and staff of affiliated hospitals involved in this project for clinical assistance. We lost our collaborator, Dr Nobuhiro Uyesaka (Department of Physiology, Nippon Medical University) during the preparation of this manuscript, and dedicate this work to honor his memory.

Conflicts of interest The authors declare that there are no conflicts of interest in relation to this manuscript.

References

1. Caimi G, Presti RL. Techniques to evaluate erythrocyte deformability in diabetes mellitus. Acta Diabetol. 2004;41:99–103.
2. Rodgers GP, Dover GJ, Uyesaka N, Noguchi CT, Schechter AN, Nienhuis AW. Augmentation by erythropoietin of the fetal-hemoglobin response to hydroxyurea in sickle cell disease. N Engl J Med. 1993;328:73–80.
3. Hiruma H, Noguchi CT, Uyesaka N, Schechter AN, Rodgers GP. Contributions of sickle hemoglobin polymer and sickle cell membranes to impaired filterability. Am J Physiol. 1995;268: H2003–8.
4. Oonishi T, Sakashita K, Uyesaka N. Regulation of red blood cell filterability by Ca^{2+} influx and cAMP-mediated signaling pathways. Am J Physiol. 1997;273:C1828–34.
5. Ariyoshi K, Maruyama T, Odashiro K, Akashi K, Fujino T, Uyesaka N. Impaired erythrocyte filterability of spontaneously hypertensive rats: investigation by nickel mesh filtration technique. Circ J. 2010;74:129–36.
6. Ejima J, Ijichi T, Ohnishi Y, Maruyama T, Kaji Y, Kanaya S, et al. Relationship of high-density lipoprotein cholesterol and red blood cell filterability: cross-sectional study of healthy subjects. Clin Hemorheol Microcirc. 2000;22:1–7.
7. Arai K, Iino M, Shio H, Uyesaka N. Further investigations of red cell deformability with nickel mesh. Biorheology. 1990;27: 47–65.
8. Nakamura T, Hasegawa S, Shio H, Uyesaka N. Rheologic and pathophysiologic significance of red cell passage through narrow pores. Blood Cells. 1994;20:151–65.
9. Mohandas N, Chasis JA. Red cell deformability, membrane material properties and shape: regulation by transmembrane, skeletal and cytosolic proteins and lipids. Semin Hematol. 1993;30:171–92.
10. Yang ZC, Xia K, Wang L, Jia SJ, Li D, Zhang Z, et al. Asymmetric dimethylarginine reduced erythrocyte deformability in streptozotocin-induced diabetic rats. Microvasc Res. 2007;73: 131–6.
11. Djemli-Shipkolye A, Raccah D, Pieroni G, Vague P, Coste TC, Gerbi A. Differential effect of omega3 PUFA supplementations on Na, K-ATPase and Mg-ATPase activities: possible role of the membrane omega6/omega3 ratio. J Membr Biol. 2003;191: 37–47.
12. Ramesh B, Pugalendi KV. Influence of umbelliferone on membrane-bound ATP_{ases} in streptozotocin-induced diabetic rats. Pharmacol Rep. 2007;59:339–48.
13. Diamantopoulos EJ, Kittas C, Charitos D, Grigoriadou M, Ifanti G, Raptis SA. Impaired erythrocyte deformability precedes vascular changes in experimental diabetes mellitus. Horm Metab Res. 2004;36:142–7.
14. Shin S, Ku YH, Suh JS, Singh M. Rheological characteristics of erythrocytes incubated in glucose media. Clin Hemorheol Microcirc. 2008;38:153–61.
15. Shin S, Ku YH, Ho JX, Kim YK, Suh JS, Singh M. Progressive impairment of erythrocyte deformability as indicator of microangiopathy in type 2 diabetes mellitus. Clin Hemorheol Microcirc. 2007;36:253–61.
16. Linderkamp O, Ruef P, Zilow EP, Hoffmann GF. Impaired deformability of erythrocytes and neutrophils in children with newly diagnosed insulin-dependent diabetes mellitus. Diabetologia. 1999;42:865–9.
17. Forst T, Weber MM, Löbig M, Lehmann U, Müller J, Hohberg C, et al. Pioglitazone in addition to metformin improves erythrocyte deformability in patients with type 2 diabetes mellitus. Clin Sci (Lond). 2010;119:345–51.
18. Satoh M, Imaizumi K, Bessho T, Shiga T. Increased erythrocyte aggregation in diabetes mellitus and its relationship to glycosylated haemoglobin and retinopathy. Diabetologia. 1984;27: 517–21.
19. Elishkevitz K, Fusman R, Koffler M, Shapira I, Zeltser D, Avitzour D, et al. Rheological determinants of red blood cell aggregation in diabetic patients in relation to their metabolic control. Diabet Med. 2002;19:152–6.
20. Uyesaka N, Hasegawa S, Ishioka N, Ishioka R, Shio H, Schechter AN. Effects of superoxide anions on red cell deformability and membrane proteins. Biorheology. 1992;29:217–29.
21. Iwata H, Ukeda H, Maruyama T, Fujino T, Sawamura M. Effect of carbonyl compounds on red blood cells deformability. Biochem Biophys Res Commun. 2004;321:700–6.
22. Okamoto K, Maruyama T, Kaji Y, Harada M, Mawatari S, Fujino T, et al. Verapamil prevents impairment in filterability of human erythrocytes exposed to oxidative stress. Jpn J Physiol. 2004;54: 39–46.
23. Mawatari S, Murakami K. Effects of ascorbate on membrane phospholipids and tocopherols of intact erythrocytes during peroxidation by *t*-butylhydroperoxide: comparison with effects of dithiothreitol. Lipids. 2001;36:57–65.

24. Ahmed FN, Naqvi FN, Shafiq F. Lipid peroxidation and serum antioxidant enzymes in patients with type 2 diabetes mellitus. Ann NY Acad Sci. 2006;1084:481–9.
25. Hansel B, Giral P, Nobecourt E, Chantepie S, Bruckert E, Chapman MJ, et al. Metabolic syndrome is associated with elevated oxidative stress and dysfunctional dense high-density lipoprotein particles displaying impaired antioxidative activity. J Clin Endocrinol Metab. 2004;89:4963–71.
26. Ford ES, Mokdad AH, Giles WH, Brown DW. The metabolic syndrome and antioxidant concentrations: findings from the Third National Health and Nutritional Examination Survey. Diabetes. 2003;52:2346–52.
27. Anichkov DA, Maksina AG, Shostak NA. Relationships between erythrocyte membrane properties and components of metabolic syndrome in women. Med Sci Monit. 2005;11:CR203–10.
28. Solá E, Vayá A, Santaolaria ML, Hernández-Mijares A, Réganon E, Vila V, et al. Erythrocyte deformability in obesity measured by ektacytometric techniques. Clin Hemorheol Microcirc. 2007;37:219–27.
29. Kraemer-Aguiar LG, Laflor CM, Bouskela E. Skin microcirculatory dysfunction is already present in normoglycemic subjects with metabolic syndrome. Metabolism. 2008;57:1740–6.
30. Grassi G, Seravalle G, Brambilla G, Facchetti R, Bolla G, Mozzi E, Mancia G. Impact of the metabolic syndrome on subcutaneous microcirculation in obese patients. J Hypertens. 2010;28:1708–14.